Progress In Electromagnetics Research C, Vol. 29, 67–81, 2012

A RECONFIGURABLE STACKED PATCH ANTENNA FOR WIRELESS POWER TRANSFER AND DATA TELEMETRY IN SENSORS

G. Yang[1], M. R. Islam[2], R. A. Dougal[2], and M. Ali[2,*]

[1]Motorola Solutions, Holtsville, New York 11742, USA

[1]Department of Electrical Engineering, University of South Carolina, Columbia, SC 29208, USA

Abstract—A reconfigurable stacked patch antenna is introduced for wireless power reception and data telemetry application in sensors. The proposed antenna operates at 5.8 GHz with 9.4 dBi gain and 7.6% bandwidth. At a lower frequency 2.45 GHz the antenna operates as a planar inverted-F antenna (PIFA) with 3.3 dBi gain and 2.0% bandwidth. Switching between the two regimes of operation is achieved using PIN diodes. It is proposed that the antenna can be used for wireless power reception in sensors at 5.8 GHz and for data telemetry in between a sensor and a control station at 2.45 GHz. The wireless power reception ability of this antenna was tested and verified by developing a high efficiency schottky diode rectifying circuit. The RF-to-DC conversion efficiency was 85% for an input power density level of 1 mW/cm^2.

1. INTRODUCTION

Reconfigurable antennas have been widely explored in defense and commercial wireless applications since a single aperture can be used to support multiple functions at separate frequency bands. Reconfigurable antennas can be realized by using MEMs or PIN diode switches. In [1] the geometry of an antenna was subdivided and MEMS switches were positioned at different locations of the antenna to change the resonant frequency. In [2] a MEMS reconfigurable Vee antenna was proposed where the beam was steered or shaped using microactuators. In conjunction with MEMS switches for reconfigurability, stacked reconfigured bow-tie elements were proposed

Received 9 February 2012, Accepted 17 April 2012, Scheduled 1 May 2012

* Corresponding author: Mohammod Ali (alimo@cec.sc.edu).

by Bernhard et al. [3] for space based radar applications. A multi-element miniature antenna was proposed in [4] which can operate at multiple frequency bands using MEMS switches. Reconfigurable patch antennas with switchable slots using PIN diodes were introduced in [5, 6]. A planar VHF reconfigurable slot antenna was loaded with multiple PIN diode switches to achieve frequency switching from 550 to 900 MHz [7]. In [8] a reconfigurable slot antenna allowing polarization switching was presented. Other reconfigurable antennas can be found in [9, 10]. Earlier we proposed a reconfigurable antenna for dual-frequency operation for satellite and land mobile radio communication applications at 2 GHz and 450 MHz, respectively [11]. An excellent review on reconfigurable antennas can be found in [12, 13]. In this paper, we propose a reconfigurable stacked microstrip patch antenna integrated with a rectifier that can function as a wideband, high gain antenna for wireless power reception in sensors at 5.8 GHz and as a data telemetry antenna at 2.45 GHz for communication in between a sensor and a local base station.

Previously we presented this concept using simulation results in [14]. In this work, we demonstrate the practical realization of that concept. Along with experimental patch and PIN diode switch measurement data measured results of wireless power transfer using a rectenna at 5.8 GHz are also presented when the rectenna is placed inside concrete samples.

Wireless power transmission in the 5–6 GHz band has been studied before in [15–24] primarily because of the band being unlicensed and that it allows larger antenna effective apertures resulting in higher antenna gain. Earlier wireless power transmission (at 5.7 GHz) to a buried sensor antenna in concrete was demonstrated in [22]. This was done considering such a scheme to charge the battery of a smart bridge health monitoring sensor.

Wireless sensors are becoming crucial for many applications ranging from infrastructure monitoring to power systems fault diagnostics. Sensors can detect a fault or problem and notify an interrogator intermittently or on a continuous basis. It is well known that once embedded inside a difficult to reach area (such as concrete) high data rate active sensors must be replenished with power wirelessly. Efficient rectenna elements if integrated with the wireless sensors can receive RF power and convert that to DC to drive the sensor circuitry. Since the sensor also needs to communicate with a nearby control station the data communication link must be established at another frequency band. In this work, we consider the 2.45 GHz band for the data telemetry function. Although a dual frequency rectenna operating at 2.45 GHz and 5.8 GHz was reported in [20] the scheme requires a

reflector plate at a distance of 17 mm from the antenna which makes the overall required volume quite large for sensor applications. On the other hand, the dual-frequency rectenna in [21] suffers from low antenna gain (3.7 dBi at 5.8 GHz).

By contrast, in this work, the stacked patch antenna when reconfigured using PIN diode switches operates as a planar inverted-F antenna [25–28] at 2.45 GHz and supports data communication between a sensor and a control station. And when reconfigured at a second frequency (5.8 GHz) works as a high gain efficient rectenna that can receive wireless power to charge a sensor battery. The reconfigurable antenna has an overall dimension of $100 \times 80 \times 6\,\text{mm}^3$ (including the rectifying circuit).

2. ANTENNA DESIGN

The reconfigurable antenna proposed here was first designed as a stacked patch for operation in the 5–6 GHz band. Fig. 1(a) shows the proposed concept. Patch 1 is printed on RO4003 (height, h_1 and dielectric constant, $\varepsilon_{r1} = 3.38$). Patch 2 is on a Rohacell foam (substrate not shown; height, h_2 and dielectric constant, $\varepsilon_{r2} = 1.04$). The antenna design was optimized for wideband operation by varying parameters h_1, h_2 and the lengths of the two patches using HFSS [29]. It was found that for $h_1 = 1.524$ mm, $h_2 = 4.5$ mm, patch lengths of $L_1 = 13$ mm and $L_2 = 17$ mm resulted in good performance for a ground plane size of 50 mm by 50 mm. The substrate extended the entire ground plane. The width, w of the transmission line was 3.5 mm. The two shorting pins in Fig. 1(b) are symmetrically positioned from both edges of Patch 2. The shorting pins are joined using a small wire. The distance between the pins is $S = 5.5$ mm. The vertical conductor

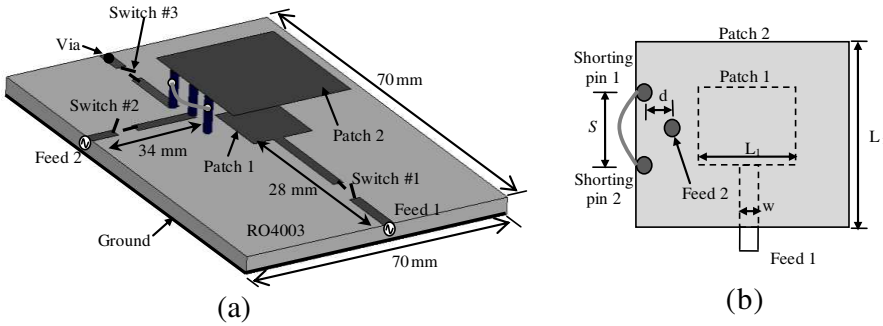

Figure 1. (a) Proposed reconfigurable antenna and (b) top view of the patches without control circuits (ground plane not shown).

for Feed 2 is located $d = 0.8$ mm inside from the edge of the patch. The diameter of the feed and shorting pin conductors is 0.5 mm.

The reconfigurable operation of the proposed antenna can be explained from Fig. 1(a). There are three switches (1, 2, and 3) that control Feed 1, Feed 2, and the shorting pins. When Feed 1 is activated (switch 1 on), Feed 2 and the shorting pins are deactivated (switches 2 and 3 are off), the antenna operates as a stacked microstrip patch at around 5.8 GHz with directional high gain beam. Next, when Feed 1 is de-activated (switch 1 is off) and Feed 2 and the shorting pins are activated (switches 2 and 3 are on) the antenna operates at 2.45 GHz with nearly omnidirectional radiation pattern.

Before having two shorting pins we observed that with only one shorting pin the PIFA resonant frequency was lower than 2.45 GHz. To ensure PIFA operation at around 2.45 GHz an additional shorting pin was added. Simulations were conducted to determine the optimum value for S. The effect of the pins and Feed 2 on stacked patch performance at 5.8 GHz was also investigated.

3. RESULTS

3.1. Reconfigurable Antenna without Control Circuits

First, operations in the stacked patch and PIFA regimes were studied without any PIN diode control circuits. Thus the switches were ideal short when activated and ideal open when deactivated. Two cases were considered:

Case 1: In the stacked patch operation (see Fig. 2(a)) Feed 1 was activated while Feed 2 and the shorting pins were deactivated. The vertical elements for Feed 2 and the two pins were connected to Patch 2 located on the top. In the bottom Feed 2 and the shorting pins touched the top surface of the RO4003 substrate. These vertical elements were modeled using cylindrical conductors (0.5 mm diameter).

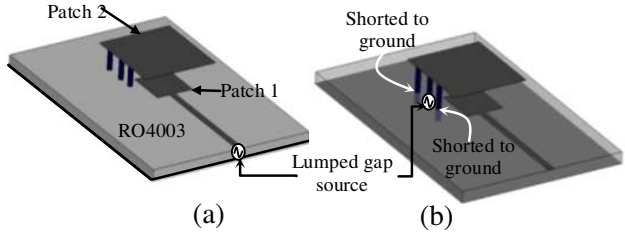

Figure 2. (a) Stacked patch mode and (b) PIFA mode without control circuits. $L_1 = 13$ mm, $L_2 = 17$ mm, $S = 5.5$ mm, $d = 0.8$ mm, ground plane: 50×50 mm^2.

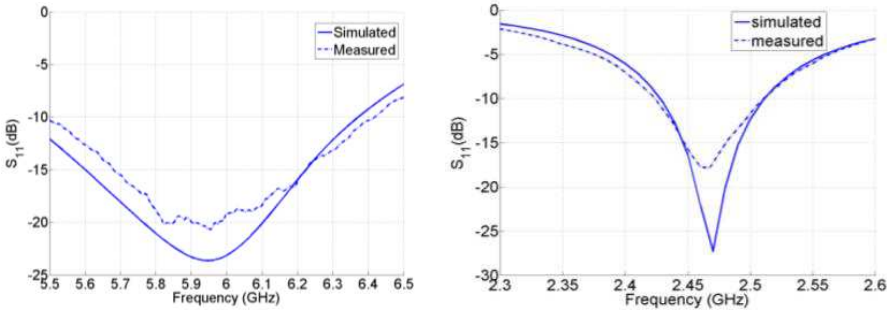

(a) (b)

Figure 3. Simulated and measured S_{11} data (dB) without control circuits; (a) stacked patch mode and (b) PIFA mode. $L_1 = 13\,\text{mm}$, $L_2 = 17\,\text{mm}$, $S = 5.5\,\text{mm}$, $d = 0.8\,\text{mm}$, ground plane: $50 \times 50\,\text{mm}^2$.

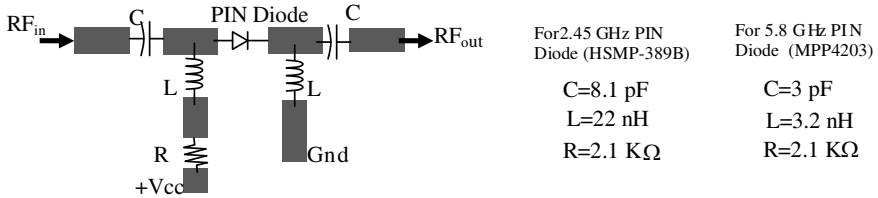

Figure 4. PIN diode control circuit.

Case 2: In the PIFA operation (see Fig. 2(b)) Feed 1 was deactivated while Feed 2 was activated and the shorting pins were directly connected to the ground below the RO4003 substrate. Simulated and measured S_{11} data for the stacked patch are shown in Fig. 3(a) (Case 1). Measured bandwidth extends from 5.5 to 6.4 GHz ($-10\,\text{dB}$). There is good agreement between the measured and simulated data. Fig. 3(b) shows the PIFA data (Case 2). Again, the simulated and measured data agree well. Measured bandwidth extends from 2.42 to 2.51 GHz.

3.2. Reconfigurable Antenna with Control Circuits

In this section, we present the results of the reconfigurable antenna containing the PIN diode switching circuits. A schematic diagram representing the switch is shown in Fig. 4. Two DC blocking Capacitors (C), two RF choke inductors (L), and a resistor (R) were used with PIN diodes to develop the switches. Switches #2 and #3 (2.45 GHz operation) were fabricated using HSMP-389B diodes from

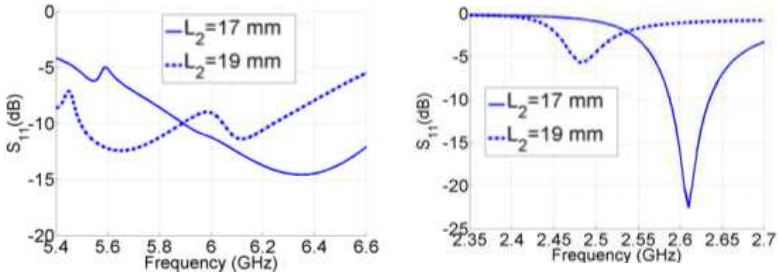

Figure 5. Simulated return loss including simple models for PIN diode control circuits with Patch 2 size (L_2) as the parameter; (a) PIFA mode, (b) patch mode. Other parameters: $L_1 = 13\,\text{mm}$, $S = 5.5\,\text{mm}$, $d = 0.8\,\text{mm}$.

Avago Technologies. Switch #1 (5.8 GHz operation) was fabricated using an MPP4203 diode from Microsemi. More details of the PIN diode switching circuits are available in [30]. At 2.45 GHz the measured insertion loss and isolation were 0.5 dB and 11 dB, respectively. Similarly at 5.8 GHz the measured insertion loss and isolation were 1.3 dB and 9.5 dB, respectively. The insertion loss and isolation are governed by the diode on resistance and off capacitance. It is expected that a 10 dB isolation will be adequate for embedded sensing applications primarily because embedded sensors will not have nearby outside interferers and the amount of power used here will be quite small to cause interference to other wireless devices even if they are nearby. If increased isolation is required very low capacitance diodes, transistors, or MEMs switches can be used.

Two simulation models were developed in HFSS to study the antenna performance with the switches. To accommodate the switching circuits the substrate and the ground plane sizes were increased from $50 \times 50\,\text{mm}^2$ to $70 \times 70\,\text{mm}^2$. In the stacked patch operation, switch #1 (Fig. 1(a)) was ON while the other two switches were OFF. All DC blocking capacitors associated with switch #1 were considered short while the inductors and the resistor associated with switch #1 were considered open. Opposite was the case for the PIFA mode. These simulations basically illustrate the effects of the transmission lines associated with the switches, the wire connecting the two shorting pins and the larger ground plane.

Simulated S_{11} data for the stacked patch and the PIFA modes for these scenarios are shown in Figs. 5(a) and (b) respectively. In the stacked patch mode, with the original dimensions ($L_2 = 17\,\text{mm}$ for Patch 2) the resonant frequency shifts from 6.0 to 6.3 GHz. Similarly,

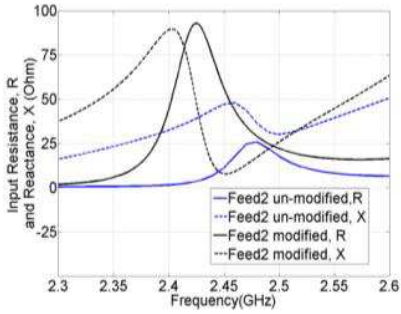

Figure 6. Simulated input resistance and reactance in the PIFA mode with and without the modification of the microstrip line Feed 2 shown in Fig. 6.

in the PIFA mode the resonant frequency moves to 2.61 GHz from 2.47 GHz. To compensate for this, Patch 2 size was increased to 19 mm. For $L_2 = 19$ mm, the stacked patch mode operates from 5.52 to 6.2 GHz. The PIFA mode operates at 2.48 GHz but the S_{11} level is poor.

To improve the PIFA S_{11} level studies of the input resistance and reactance of the PIFA mode (Fig. 6) show that the input reactance at 2.45 GHz is about $+j47\Omega$. To reduce this reactance, modifications were made near the PIFA feed. Figs. 7(a) and (b) also show the surface current plots at 2.45 GHz for the un-modified and modified feed models. Clearly in Fig. 7(b) there is more current concentration than the un-modified feed in Fig. 7(a). This translates into additional capacitance which causes the input reactance to decrease from $+j47\,\Omega$ to $+j2.9\,\Omega$ (Fig. 6). As shown in Fig. 7(b) the modified feed had S= 4.7 mm and $d = 1.8$ mm compared to $S = 5.5$ mm and $d = 0.8$ mm for the un-modified feed. These adjustments also increased the input resistance from $11.2\,\Omega$ to $50.3\,\Omega$. Based on these modifications we fabricated our final reconfigurable antenna prototype and measured it before the rectifying circuitry was added.

To understand the effect of the switches on the antenna S_{11} and gain, we also modeled and simulated the reconfigurable antenna in Designer [29]. Figs. 8(a)–(b) show these models. First, we measured the S parameters of the 2.45 GHz and 5.8 GHz switching circuits and then saved those data in two separate s2p files which were loaded in Designer. Note that, in Designer simulations there were no transmission lines connected with the feeds (Figs. 8(a)–(b)). This was done to eliminate the delay associated with the transmission lines present in the fabricated prototype of the switching circuits (the

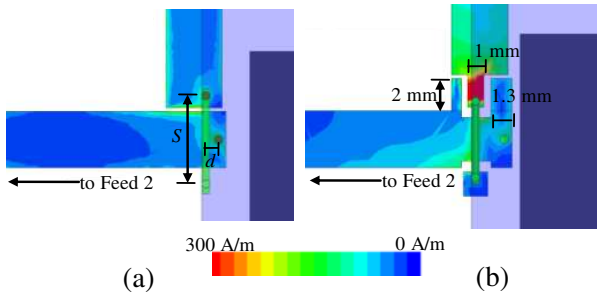

Figure 7. Simulated surface current plot for the (a) un-modified model, $S = 5.5\,\text{mm}$, $d = 0.8\,\text{mm}$ and the (b) modified model, $S = 4.7\,\text{mm}$, $d = 1.8\,\text{mm}$. Other parameters: $L_1 = 13\,\text{mm}$, $L_2 = 19\,\text{mm}$.

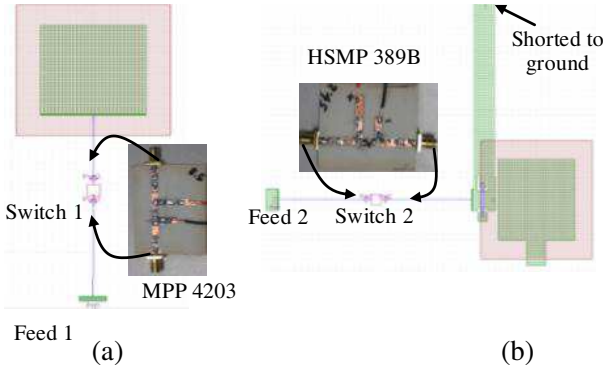

Figure 8. Designer simulation model with switch; (a) stacked patch mode and (b) PIFA mode.

prototypes are also shown in Fig. 8). Since there was no signal source connected with switch #3, it was replaced by a transmission line section to ensure the PIFA mode emulation in Designer.

Measured results are shown in Fig. 9. For comparison, data simulated with HFSS and Designer are also shown in Fig. 9. In Fig. 9 with switches #2 and #3 in the 'OFF' state and switch #1 in the 'ON' state the antenna operates from 5.57 to 6.01 GHz, bandwidth = 7.6% (Fig. 9(a)). This bandwidth is narrower than the measured stacked patch bandwidth without control circuits (Fig. 3(a)). This may be due to the impedance mismatch between the switch and the stacked patch. In general, the measured data are in agreement with the Designer simulated data. Slight discrepancy can be attributed to the fact that Designer considers infinite substrate and infinite ground plane whereas the experimental prototype and HFSS models represent finite substrate and finite ground plane.

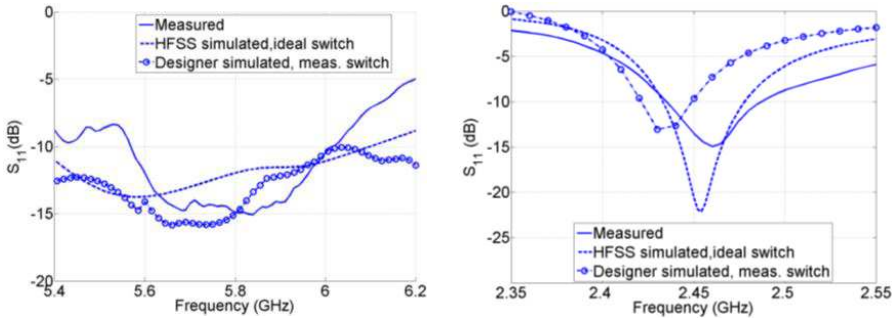

Figure 9. Measured and simulated impedance bandwidth of the reconfigurable antenna with the PIN diode circuits; (a) stacked patch and (b) PIFA mode. $L_1 = 13\,\text{mm}$, $L_2 = 19\,\text{mm}$, $S = 4.7\,\text{mm}$, $d = 1.8\,\text{mm}$, Feed 2 modified.

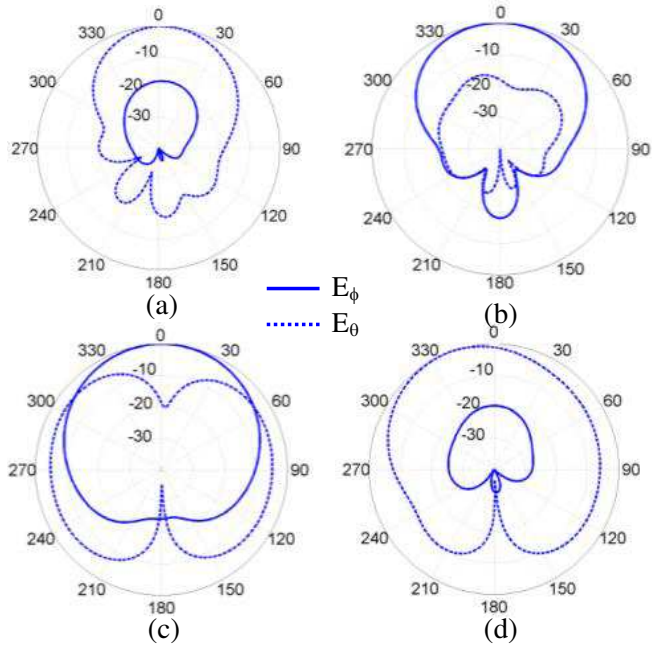

Figure 10. Simulated normalized radiation patterns with simple PIN diode control circuit models; (a) E plane ($\phi = 0°$) at 5.8 GHz, (b) H plane ($\phi = 90°$) at 5.8 GHz, (c) $\phi = 0°$ at 2.45 GHz, and (d) $\phi = 90°$ at 2.45 GHz.

With switch #1 in the 'OFF' state and switches #2 and #3 in the 'ON' state we have the PIFA mode operation for which the measured data are shown in Fig. 9(b). The bandwidth extends from 2.43 to 2.48 GHz (2.0%). The measured data agree well with the simulations. The levels of measured S_{11} compare quite well with those obtained using Designer. Slight detuning in the Designer simulated data is observed because designer considers infinite substrate and infinite ground plane.

Simulated radiation patterns (using HFSS) of the PIFA and the stacked patch modes ($L_1 = 13\,\text{mm}$, $L_2 = 19\,\text{mm}$, $S = 4.7\,\text{mm}$, $d = 1.8\,\text{mm}$, feed and shorting pin region modified) are shown in Fig. 10. Figs. 10(a) ($\phi = 0°$, E plane) and 10(b) ($\phi = 90°$, H plane) illustrate the patterns at 5.8 GHz. The peak realized gain is 9.4 dBi not including the switch insertion loss. To determine the effect of switch loss on antenna gain degradation two simulations were performed in Designer one with the switch and the other without the switch. Peak gain decreased by 1.3 dB with the switch. Thus the peak gain in the stacked patch mode is 8.1 dBi. Fig. 10(c) ($\phi = 0°$) and 10(d) ($\phi = 90°$) depict the patterns (HFSS) at 2.45 GHz, for the PIFA mode. They are standard PIFA radiation patterns with 3.3 dBi peak gain not including switch losses. Designer simulations show 0.4 dB gain reduction at 2.45 GHz. Thus, the peak gain in the PIFA mode is 2.9 dBi.

4. APPLICATION OF RECONFIGURABLE ANTENNA FOR WIRELESS POWER TRANSMISSION

To test the wireless power reception ability of the proposed antenna, a rectifying circuit was fabricated and connected to the stacked reconfigurable patch as shown in Fig. 11. The rectifier consisted of an HSMS-2862 microwave Si Schottky detector diode pair ($R_s = 6.0\,\Omega$, $C_{j0} = 0.18\,\text{pF}$, $V_{bi} = 0.65\,\text{V}$, and $V_B = 7\,\text{V}$ for each diode), a capacitor C and a load resistor R_L. The equivalent circuit parameters are given in [15]. The diode pair was connected as a voltage-doubler to increase the output DC voltage (V_D). A quarter wave length transformer T_1 ($1.95\,\text{mm} \times 7\,\text{mm}$) and a microstrip line T_2 ($0.94\,\text{mm} \times 3\,\text{mm}$) were used between the diode pair and the antenna for impedance matching (Fig. 11). Detail description of the rectifying circuit can be found in [30].

The performance of the rectenna was measured by illuminating it with a four-element microstrip patch antenna array (13.6 dBi gain) described in [22] which was connected to a high-power amplifier (7 W, 5.3–5.9 GHz) and a microwave signal generator. The received voltage at the rectenna was measured using a voltmeter. The transmitter

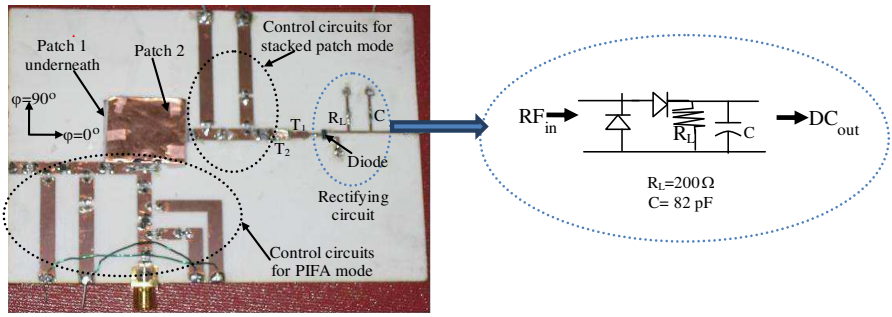

Figure 11. Fabricated reconfigurable antenna and rectifying circuit, ground plane size: $100 \times 80\,\text{mm}^2$.

antenna array and the rectenna were separated by distance, r. The smallest distance was 60 cm which satisfied the far-field condition of radiation $(2r^2/\lambda)$ at 5.8 GHz.

The rectenna RF-to-DC conversion efficiency was calculated as [15],

$$\eta_R = \frac{\left(\frac{V_D^2}{R_L}\right)}{P_t G_r G_t \left(\frac{\lambda_0}{4\pi r}\right)^2}$$

where P_t and G_t represent the transmit power and transmitting array antenna's gain, G_r represents the gain of the rectenna, V_D is the voltage across the load resistor R_L. Here frequency was 5.8 GHz, $G_t = 13.6\,\text{dBi}$, $G_r = 8.1\,\text{dBi}$, and $P_t = 7\,\text{W}$. Measured V_D versus r is shown in Fig. 12(a). The rectenna received 3 V DC. The rectenna conversion efficiency was 85.5% with an incident power density of $1\,\text{mW/cm}^2$. The conversion efficiency data shown in Fig. 12(b) was plotted using the discrete measured voltage data. For power densities lower than $0.75\,\text{mW/cm}^2$ the conversion efficiency decreases rapidly. This is because a certain amount of power is required to turn the rectifying diode pair on and also to trade the switch insertion loss off. When the incident power density is lower than this certain level, the voltage across R_L is very low resulting in low conversion efficiency. The minor ripples observed in Fig. 12(b) may have been caused due to undesirable reflections.

To study the feasibility of the proposed scheme for a practical application, two additional experiments were performed where the reconfigurable rectenna was placed inside dry concrete blocks ($500\,\text{mm} \times 500\,\text{mm} \times 25\,\text{mm}$). The rectenna was placed underneath two 25 mm thick concrete blocks as shown in Fig. 13(a). A transmit

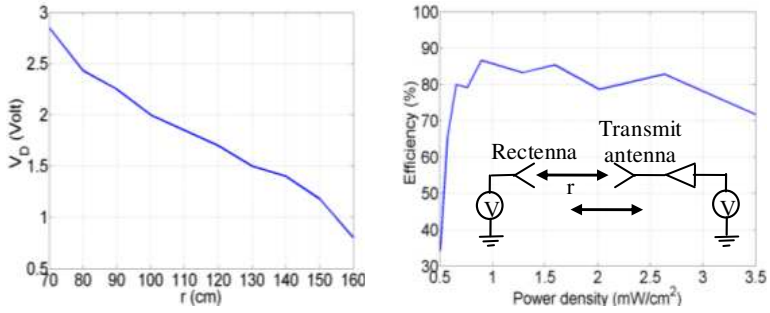

(a) (b)

Figure 12. Measured output voltage V_D and conversion efficiency at 5.8 GHz; (a) V_D versus distance r, (b) conversion efficiency versus power density; $R_L = 200\,\Omega$, $C = 82\,\text{pF}$.

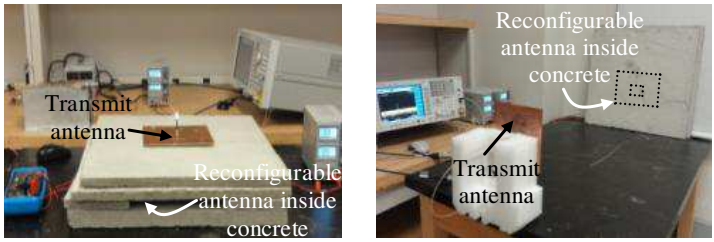

(a) (b)

Figure 13. Experimental setup for (a) power transfer through concrete at 5.8 GHz and (b) wireless communication through concrete at 2.45 GHz.

patch array was placed right against the concrete as shown. At 5.8 GHz (Fig. 13(a)) the rectifier output was 2.1 V DC when the reconfigurable antenna was illuminated using the transmit patch array. Thus clearly the reconfigurable mode of operation can be used to charge the battery of an embedded wireless sensor in concrete.

In the other experiment conducted at 2.45 GHz, the transmitter-receiver separation was 1 m. A single patch antenna (10 dBi) was used as the transmitter while the reconfigurable antenna in the PIFA mode was used as the receiver which was placed behind two 25 mm thick concrete blocks (Fig. 13(b)). The receive signal level at 2.45 GHz was -39.2 dBm when the transmit power was $+10$ dBm. Considering the Friis transmission formula we estimate that the reconfigurable antenna at 2.45 GHz will be able to reliably communicate with a nearby base station transmitting $+10$ dBm at 100 m distance where the received signal strength will be about -80 dBm which is much higher than the sensitivity of most receivers at that frequency.

5. CONCLUSION

The study and design of a stacked reconfigurable microstrip patch antenna are presented. Using PIN diode switches it is demonstrated that a stacked microstrip patch can be reconfigured to support two distinctly different operating frequency bands with varying bandwidth and radiation patterns. The stacked patch is suitable for wireless power reception in sensors. The PIFA is suitable for wireless data communication between sensors or sensor and a control station due to its balanced azimuthal pattern coverage. The reconfigurable antenna when integrated with a rectifying circuit can receive and convert RF energy with a conversion efficiency of 85%. The reconfigurable antenna can successfully receive power and communicate with nearby base station when it is embedded in concrete.

ACKNOWLEDGMENT

This work was supported in part by the US Office of Naval Research under grant No. 0014-02-1-0623.

REFERENCES

1. Weedon, W. H. and W. J. Payne, "MEMS-switched reconfigurable multi-band antenna: Design and modeling," *Proceedings of the 1999 Antenna Applications Symposium*, Monticello, IL, Sep. 15–17, 1999.
2. Chiao, J.-C., Y. Fu, I. M. Chio, M. D. Lisio, and L. Y. Lin, "MEMS reconfigurable vee antenna," *IEEE MTT-S Symp. Dig.*, 1999.
3. Bernhard, J. T., R. Wang, and P. Mayes, "Stacked reconfigurable antenna elements for space based radar applications," *IEEE Antennas Propagat. Symp. Dig.*, Vol. 1, 158–161, 2001.
4. Jofre, L., B. A. Cetiner, and F. de Falviss, "Miniature multi-element antenna for wireless communications," *IEEE Trans. Antennas Propagat.,* Vol. 50, 658–669, May 2002.
5. Yang, F. and Y. Rahmat-Samii, "Patch antenna with switchable slot (PASS): Dual frequency operation," *Microwave Opt. Technol. Lett.,* Vol. 31, No. 3, 165–168, Nov. 2001.
6. Yang, F. and Y. Rahmat-Samii, "A reconfigurable patch antenna using switchable slots for circular polarization diversity," *IEEE Microwave Wireless Component Lett.,* Vol. 12, 96–98, Mar. 2002.

7. Peroulis, D., K. Sarabandi, and L. P. B. Katehi, "A planar VHF reconfigurable slot antenna," *IEEE Antennas Propagat. Symp. Dig.*, Vol. 1, 154–157, 2001.
8. Fries, M. K., M. Grani, and R. Vahldieck, "A reconfigurable slot antenna with switchable polarization," *IEEE Microwave Wireless Component Lett.*, Vol. 13, 490–492, Nov. 2003.
9. Langer, J. C., J. Zou, C. Liu, and J. T. Bernhard, "Micromachined reconfigurable out-of-plane microstrip patch antenna using plastic deformation magnetic actuation," *IEEE Microwave Wireless Component Lett.*, Vol. 13, 120–122, Mar. 2003.
10. Nair, S. V. S. and M. J. Ammann, "Reconfigurable antenna with elevation and azimuth beam switching," *IEEE Antennas Wireless Propagat. Lett.*, Vol. 9, 367–370, 2010.
11. Kunda, V. K., M. Ali, and H. S. Hwang, "A tunable stacked microstrip patch antenna for directional and omnidirectional links," *Proc. IEEE Antennas and Propagation Society International Symposium and URSI/USNC Meeting*, Monterey, CA, Jun. 2004.
12. Bernhard, J. T., "Reconfigurable antennas," *The Wiley Encyclopedia of RF and Microwave Engineering*, K. Chang, Editor, 2005.
13. Bernhard, J. T., "Reconfigurable antennas," *Antenna Engineering Handbook*, J. Volakis, Editor, 4th Edition, McGraw Hill, 2007.
14. Yang, G., M. Ali, and R. A. Dougal, "A multi-functional stacked patch antenna for wireless power beaming and data telemetry," *Proc. IEEE Antennas and Propagat. Soc. Int. Sym. Dig.,* Vol. 2A, 359–362, Washington, DC, Jul. 2005.
15. Strassner, B. and K. Chang, "5.8 GHz circularly polarized rectifying antenna for wireless microwave power transmission," *IEEE Trans. Microwave Theory Tech.*, Vol. 50, 1870–1876, Aug. 2002.
16. Strassner, B. and K. Chang, "5.8 GHz circularly polarized dual-rhombic-loop traveling-wave rectifying antenna for low power-density wireless power transmission applications," *IEEE Trans. Microwave Theory Tech.*, Vol. 51, 1548–1553, May 2003.
17. Chin, C. K., Q. Xue, and C. H. Chan, "Design of a 5.8-GHz rectenna incorporating a new patch antenna," *IEEE Antennas Wireless Propagat. Lett.*, Vol. 4, 175–178, 2005.
18. Ren, Y. and K. Chang, "5.8 GHz circularly polarized dual-diode rectenna and rectenna array for microwave power transmission," *IEEE Trans. Microwave Theory Tech.*, Vol. 54, 1495–1502, Apr. 2006.

19. Radiom, S., M. B. Nejad, K. M. Aghdam, G. A. E. Vandenbosch, L. Zheng, and G. G. E. Gielen, "Far-field on-chip antennas monolithically integrated in a wireless-powered 5.8-GHz downlink/UWB uplink RFID tag in 0.18-µm standard CMOS," *IEEE Journal. Solid State Cir.*, Vol. 45, 1746–1758, Sep. 2010.
20. Suh, Y. and K. Chang, "A high-efficiency dual-frequency rectenna for 2.45- and 5.8-GHz wireless power transmission," *IEEE Trans. Microwave Theory Tech.*, Vol. 50, 1784–1789, Jul. 2002.
21. Heikkinen, J. and M. Kivikoski, "A novel dual-frequency circularly polarized rectenna," *IEEE Antennas Wireless Propagat. Lett.*, Vol. 2, 330–333, 2003.
22. Shams, K. M. Z. and M. Ali, "Wireless power transmission to a buried sensor in concrete," *IEEE Sensors Journal*, Vol. 7, 1573–1577, Dec. 2007.
23. Ali, M., G. Yang, and R. A. Dougal, "A new circularly polarized rectenna for wireless power transmission and data communication," *IEEE Antennas Wireless Propagat. Lett.*, Vol. 4, 205–208, Jul. 2005.
24. Ali, M., G. Yang, and R. Dougal, "Miniature circularly polarized rectenna with reduced out of band harmonics," *IEEE Antennas and Wireless Propagat. Lett.*, Vol. 5, 107–110, 2006.
25. Rowell, C. R. and R. D. Murch, "A capacitively loaded PIFA for compact mobile telephone handsets," *IEEE Trans. Antennas Propagat.,* Vol. 45, 837–842, May 1997.
26. Virga, K. L. and Y. Rahmat-Samii, "Low-profile enhanced-bandwidth PIFA antennas for wireless communications packaging," *IEEE Trans. Microwave Theory Tech.*, Vol. 45, 1879–1888, Oct. 1997.
27. Waterhouse, R. B., S. D. Targonski, and D. M. Kokotoff, "Design and performance of small printed antennas," *IEEE Trans. Antennas Propagat.*, Vol. 46, 1629–1633, Nov. 1998.
28. Karmakar, N. C., "Shorting strap tunable stacked patch PIFA," *IEEE Trans. Antennas Propagat.*, Vol. 52, 2877–2884, Nov. 2004.
29. Ansoft Corporation, Available: www.ansoft.com.
30. Yang, G., "Conformal multi-functional antennas and rectifying circuits for wireless communication and microwave power beaming," Ph.D. Dissertation, University of South Carolina, 2005.